Predictive Models of Resting State Networks for Assessment of Altered Functional Connectivity in MCI

Xi Jiang[1], Dajiang Zhu[1], Kaiming Li[2], Tuo Zhang[3,1], Dinggang Shen[4], Lei Guo[3], and Tianming Liu[1]

[1] Cortical Architecture Imaging and Discovery Lab, Department of Computer Science and Bioimaging Research Center, The University of Georgia, Athens, GA, USA
[2] Biomedical Imaging Technology Center, Emory University/Georgia Institute of Technology, Atlanta, GA, USA
[3] School of Automation, Northwestern Polytechnical University, Xi'an, China
[4] Department of Radiology, UNC Chapel Hill, NC, USA

Abstract. Due to the difficulties in establishing accurate correspondences of brain network nodes across individual subjects, systematic elucidation of possible functional connectivity (FC) alterations in mild cognitive impairment (MCI) compared with normal controls (NC) is a challenging problem. To address this challenge, in this paper, we develop and apply novel predictive models of resting state networks (RSNs) learned from multimodal resting state fMRI (R-fMRI) and DTI data to assess large-scale FC alterations in MCI. Our rationale is that some RSNs in MCI are substantially altered and can hardly be directly compared with those in NC. Instead, structural landmarks derived from DTI data are much more consistent and correspondent across MCI/NC brains, and therefore can be employed to encode RSNs in NC and serve as the predictive models of RSNs for MCI. To derive these predictive models, RSNs in NC are constructed by group-wise ICA clustering and employed to functionally annotate corresponding structural landmarks. Afterwards, these functionally-annotated structural landmarks are predicted in MCI based on DTI data and used to assess FC alterations in MCI. Experimental results demonstrated that the predictive models of RSNs are effective and can comprehensively reveal widespread FC alterations in MCI.

Keywords: mild cognitive impairment (MCI), resting state networks, predictive models, functional connectivity (FC).

1 Introduction

Recent studies have shown that mild cognitive impairment (MCI), which is the precursor of Alzheimer's disease (AD), exhibits widespread alterations in functional brain networks as revealed by resting state f-fMRI (R-fMRI) data [2-3]. Therefore, there has been increasingly significant effort in measuring the hypothesized widespread functional connectivity (FC) alterations within the brain networks in MCI. However, a fundamental, challenging issue in FC analysis is how to accurately localize brain network nodes across different subjects and populations. Existing

K. Mori et al. (Eds.): MICCAI 2013, Part II, LNCS 8150, pp. 674–681, 2013.

approaches to identifying network nodes, or regions of interests (ROIs), for FC analysis can be broadly classified into four categories: manually labeling by experts based on their domain knowledge [1-2], data-driven clustering such as independent component analysis (ICA) [4] and regional homogeneity (ReHo) [5], warping predefined landmarks in the template brain to individual space using image registration algorithms [6], and identifying activated brain regions based on task-based fMRI.

However, the abovementioned methods might be suboptimal for assessing large-scale FC alterations in MCI since certain RSNs in MCI are possibly disrupted or missing along with the disease progression [7]. That is, some altered RSNs in MCI can hardly be directly compared with those normal RSNs in NC, and thus the localization of corresponding brain network nodes across MCI and NC subjects is considerably challenging. To demonstrate this point, Figs. 1A-1O shows 15 group-wise RSNs identified in NC using group-ICA clustering [8]. In comparison, only 10 roughly corresponding RSNs are identified in MCI and the other five RSNs are missing or substantially altered, as shown in Figs. 1A'-1O'. The missing or altered RSNs in MCI make it difficult to quantitatively assess and compare large-scale FC in MCI with that in NC, given the lack of corresponding RSN nodes across MCI and NC populations.

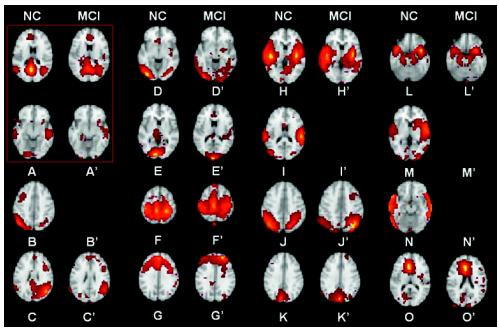

Fig. 1. Visualization of 15 RSNs in NC (A-O) and MCI (A'-O'). All 15 ICA components are shown on a T1-weighted structural MRI image. 4 RSNs in NC (B, I, M and N) are missing in MCI and 1 RSN in MCI (A') is altered. The color scale represents z values ranging from 0 to 23.1. More interpretations are provided in Section 3.1.

Fortunately, our extensive experimental observations have shown that the structural landmarks derived from DTI in MCI are relatively intact compared to those in NC (more details in Section 3.2). Thus, in this paper, we tackle the challenge of localizing corresponding network nodes in MCI by using a publicly available cortical landmarks system DICCCOL (Dense Individualized and Common Connectivity-based Cortical Landmarks) [9]. The neuroscience basis of the DICCCOL is that each brain's cytoarchitectonic area has a unique set of extrinsic inputs/outputs, named the "connectional fingerprint" [10], which principally determine the functions that each brain area could possibly possess. A prominent characteristic of the DICCCOL system is that it offers 358 common structural cortical landmarks that are defined by group-wise consistent fiber connection patterns [9] (more details in Section 2.3). The 358 DICCCOLs have been reproducible in over 240 healthy brains and can be quite accurately predicted in each individual brain based on DTI data [9].

Therefore, in this paper, the DICCCOL system is employed to encode RSNs in NC and serve as the predictive models of RSNs for MCI. To develop the predictive models, RSNs in NC brains are constructed by group-wise ICA clustering [8] and

employed to functionally annotate the corresponding structural landmarks within a group of NC brains. In the application stage, these functionally-annotated structural DICCCOL landmarks are predicted in MCI brains based on DTI data and used to assess large-scale FC alterations in MCI. The contribution of this paper is that DICCCOLs that are structurally consistent in both NC and MCI were applied as predictive models of RSNs to assess functional connectivity alterations in MCI. These predictive models of RSNs effectively leverage the machine learning paradigm and provide a novel solution to the challenging problem of accurately localizing corresponding network nodes ROIs in brain conditions (MCI in this work).

2 Materials and Methods

2.1 Overview

The flowchart of developing and applying predictive models of RSNs is illustrated in Fig. 2. It consists of four major steps. In step 1, group-ICA was applied to construct RSNs from R-fMRI data in NC. In step 2, DICCCOLs were predicted in both NC and MCI. In step 3, predictive models of RSNs were learned in the NC group, and in step 4, the learned predictive models of RSNs were applied in MCI for FC alteration assessment.

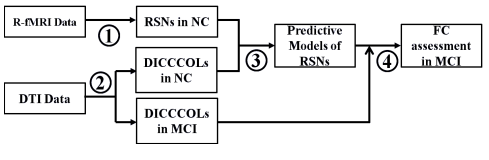

Fig. 2. The flowchart of developing and applying predictive models of RSNs

2.2 Data Acquisition and Preprocessing

Twenty-eight participants (10 MCI and 18 socio-demographically matched NC) were scanned in a 3.0 Tesla scanner (GE Signa EXCITE). For DTI, 25 direction diffusion-weighted whole-brain volumes were acquired axially parallel to the AC-PC line, with b = 0 and 1000 s/mm2, flip angle = 90°, TR = 17 s and TE = 78 ms. The imaging matrix is 256 x 256 with a rectangular FOV of 256 x 256 mm2 and 72 slices with a slice thickness of 2.0 mm. For R-fMRI, 34 slices were acquired in the same plane using a SENSE inverse-spiral pulse sequence with echo time (TE) = 32 ms, repetition time (TR) = 2000 ms, FOV = 25.6 cm2, matrix = 64 × 64 × 34, 3.8 mm3. Pre-processing steps of the R-fMRI and DTI are referred to [9].

2.3 Construction of RSNs in NC and Prediction of DICCCOLs

We identified RSNs in NC by using the group-ICA implemented in the GIFT toolbox [8, 11]. In brief, first, we constructed subject-specific components based on R-fMRI data. Second, by using the brain templates available in the GIFT toolbox, we determined corresponding group mean independent components that represent RSNs

elaborated in previous RSN studies [4, 7, 12-13] and excluded other components that are deemed to be artifacts, i.e., in ventricle or cerebrospinal fluid (CSF).

Next, the DICCCOL prediction procedure [9] was applied on the NC and MCI brains with DTI data. Briefly, the DICCCOL prediction was formulated as an optimization problem. We first generated dense and corresponding landmarks on the reconstructed cortical surfaces based on DTI data across subjects. We then extracted white matter fiber bundles emanating from small regions of each landmark. Each region served as the candidate for landmark location optimization. Afterwards, we used trace-map model [9], which is represented as a 144-dimenional vector, to quantitatively describe the fiber bundles and calculated the distance between any pair of trace-maps in different subjects. For each corresponding landmark, we performed a whole-space search to find fiber bundles which gave the best group-wise similarity. Finally, we determined 358 DICCCOL landmarks which possess group-wise consistency of fiber shape patterns in both the NC and MCI brains.

2.4 Predictive Models of RSNs Based on DICCCOLs

The constructed RSNs and predicted DICCCOLs in NC brains in the above section are used to learn predictive models of RSNs as follows. First, the activity peaks (represented by z-values) of each RSN were selected in NC to represent the corresponding RSNs. Then, for each corresponding activity peak in NC group, the top 5 closest DICCCOLs (measured by Euclidian distance) in each subject were identified out of the 358 candidates. Second, the DICCCOL landmarks with the most votes (defined as frequencies of being ranked as closest to current activity peak within the group) was determined as the predictive landmark for the current activity peak. Therefore, we encoded all 15 RSNs in NC (Fig.1) via DICCCOLs and used those DICCCOLs as predictive models of RSNs. Since the structural brain architectures in MCI are relative intact compared to those in NC (Section 3.2), FC was assessed based on the predicted RSNs in MCI and compared with that in NC.

3 Experimental Results

3.1 Construction of RSNs in NC

Results of the constructed RSNs in NC are already depicted in Figs. 1A-1O. In total, 15 RSNs were identified, as shown in Figs. 1A-1O. Specifically, Fig. 1A includes the medial prefrontal gyrus (BAs (Brodmann Area) 9/10/11), anterior (BAs 12/32) and posterior cingulate cortex (BA 29), bilateral supramarginal gyrus (BA 39), and the inferior temporal gyrus (BA 21), which corresponds to the default mode network (DMN) [7, 12-13]. The components of other RSNs in Figs. 1B-1O are similar to those in [4, 7, 12-13]. All activity peaks of RSNs in NC were then selected. Fig. 5a visualizes all 38 peaks in 15 RSNs. Moreover, RSNs in MCI were reconstructed for comparison. As shown in Figs. 1A'-1O', only 10 corresponding RSNs were identified in MCI and the other 5 RSNs were missing or substantially altered, including the DMN. These disrupted or missing RSNs in MCI make it very challenging to assess FC in MCI with that in NC, thus warranting the predictive models of RSNs via DICCCOLs.

3.2 Consistency of DICCCOLs in NC and MCI

We qualitatively and quantitatively compared the fiber patterns of the 358 predicted DICCCOLs in both NC and MCI to verify the structural intactness of DICCCOLs in MCI. Figs. 3a-3b show two examples of corresponding DICCCOLs (#311 and #315, as indexed in [9]) in the original healthy model brains, NC and MCI, respectively. In each sub-figure, rows 1-3 are three exemplar model brains, NC and MCI brains, respectively.

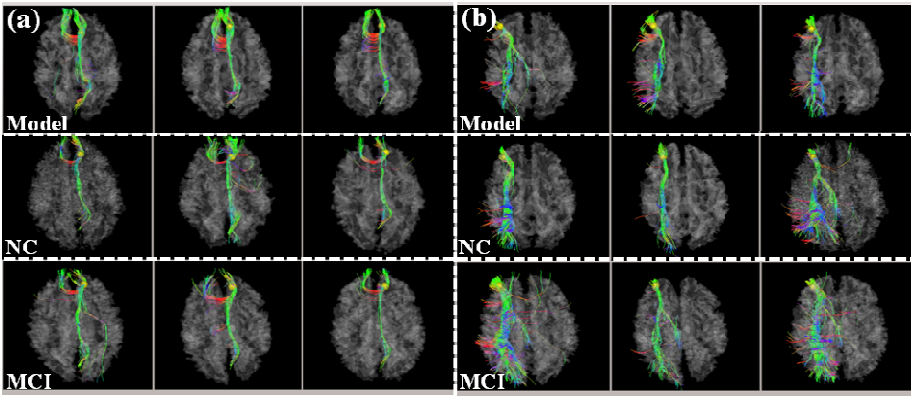

Fig. 3. Two example DICCCOLs in model brains, NC and MCI

From visual inspection, the fiber shape patterns of corresponding DICCCOLs are similar to those in models/NC/MCI. Quantitatively, we calculated the distances of the mean trace-maps [9] of 358 DICCCOLs between any two of the three groups (models, NC and MCI) via the same method in [9]. As shown in Table 1 (shading white), the distances of the mean trace-maps of 5 randomly selected DICCCOLs between any two groups are all very small: 28.46×10-5, 23.16×10-5, and 5.04×10-5. To further demonstrate that the above distances are indeed small, we randomly selected 5 vertices on the entire cortical surface of one model, extracted their fiber bundles, and calculated the distances of the trace-maps between each of the five and DICCCOL #327 as an example. As shown in Table 1 (shading gray), the mean distance is 254.26×10-5 which is obviously much larger than the above three distances. For all of the rest DICCCOLs, we have the similar finding, suggesting that the DICCCOLs well represent structural connectivity patterns in MCI, which is also the foundation that we can use DICCCOLs to encode RSNs and apply them as predictive models to assess FC alterations in MCI.

Table 1. Distances ($\times 10^{-5}$) of mean trace-maps of DICCCOLs between models (M), NC and MCI

ID	**#327**	**#77**	**#145**	**#46**	**#303**	**Mean**
M – NC	35.29	14.11	20.62	33.41	38.88	**28.46**
M – MCI	24.19	15.66	18.91	22.97	34.05	**23.16**
NC – MCI	8.66	5.75	1.96	4.29	4.52	**5.04**
Vertex	**#1**	**#2**	**#3**	**#4**	**#5**	**Mean**
Distance	197.97	424.49	251.96	241.75	155.14	**254.26**

3.3 Predictive Models of RSNs Based on DICCCOLs

Fig. 4a visualizes all 38 activity peaks of 15 RSNs in NC and their corresponding encoded DICCCOLs in one NC brain. Fig. 4b shows the DICCCOL-based predicted RSNs in one MCI brain. To quantitatively evaluate the encoding accuracy of RSNs by DICCCOLs, we measured and reported the mean Euclidean distance between the centers of activity peaks within each RSN and corresponding encoded DICCCOLs in NC, respectively in Table 2. We also calculated the mean geodesic distance was also calculated and result is 6.11 mm. The results demonstrate that DICCCOLs are consistently co-localized with RSNs, and can encode RSNs effectively and accurately.

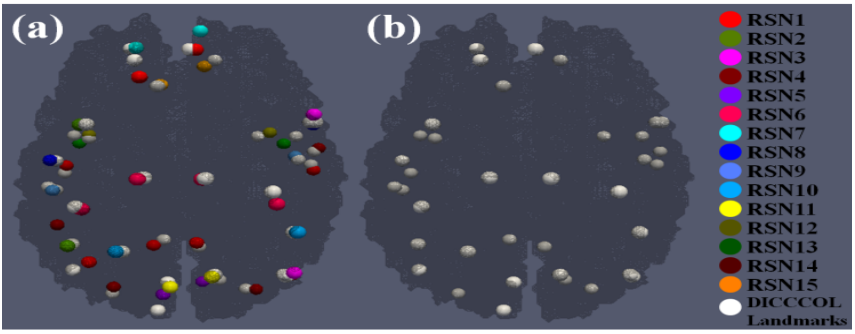

Fig. 4. Predictive models of RSN. (a) All 38 activity peaks of 15 RSNs and encoded DICCCOLs in NC; (b) DICCCOL-based predicted RSNs in MCI. Activity peaks in different RSNs are represented by the bubbles with different colors in the right panel. DICCCOLs are represented by the white bubbles.

Table 2. Mean Euclidean distance (mm) between the centers of activity peaks within each RSN and encoded DICCCOLs

RSN	**#1**	**#2**	**#3**	**#4**	**#5**	**#6**	**#7**	**#8**
Distance	5.54	5.99	4.86	7.31	8.79	4.11	5.39	6.02
RSN	**#9**	**#10**	**#11**	**#12**	**#13**	**#14**	**#15**	**Mean**
Distance	4.92	5.99	5.91	5.54	5.60	5.51	5.73	**5.81**

3.4 FC in NC and MCI

First, we verified that FC based on (i) activity peaks of RSNs and (ii) DICCCOL-based predictive models of RSNs were similar in NC. The FC between two peaks/DICCCOLs was defined as the Pearson correlation coefficient between their representative R-fMRI time series. As shown in Figs. 5a-5b, the average FC based on (i) and (ii) are similar, as highlighted by the white frames in the principal diagonal direction. Furthermore, for some RSNs (#9, 13 and 14), the average FC based on (ii) is even higher than that based on (i), suggesting that the DICCCOLs might help localize individual RSNs more accurately than using the ICA approach. This is in agreement with previous results [14] that group-wise consistency of structural connection patterns of functional landmarks could benefit FC profile.

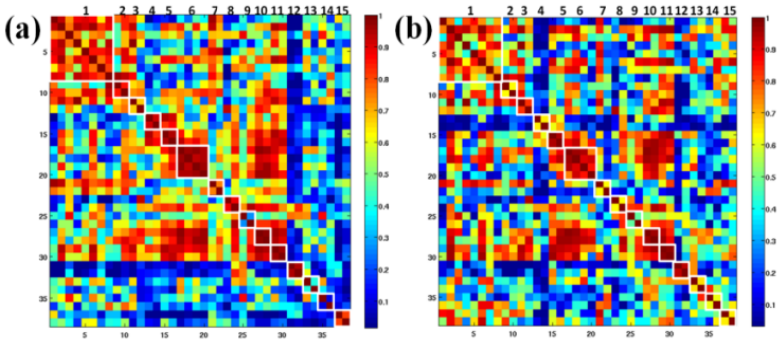

Fig. 5. Average FC based on (a) activity peaks of RSNs and (b) DICCCOL-based predictive models, respectively. RSNs are highlighted by the white frames in the principal diagonal direction and indexed in the top panel.

Second, we used the predictive models to assess FC in MCI compared with that in NC. Figs. 6a-6b show the average FC based on the predictive models of RSNs in NC and MCI, respectively. We can see that FC is substantially different between NC and MCI. To statistically examine the significance of between-group difference, we performed a two-sample t-test of FC in Figs. 6a-6b. Significantly decreased (blue) and increased (red) (p=0.05) FCs in MCI compared to NC are shown in Figs. 6c-6d,

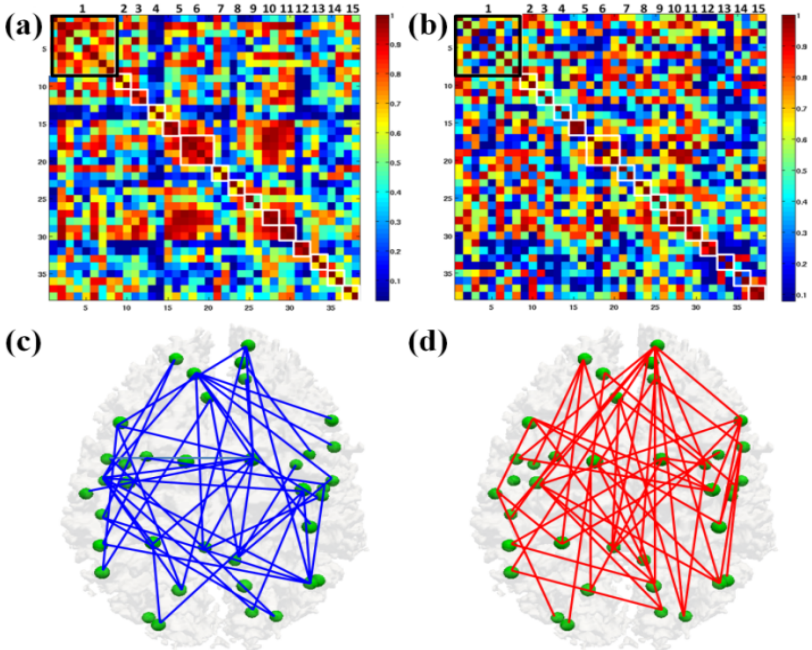

Fig. 6. Widespread FC alterations in MCI. (a)-(b) represent average FC based on the DICCCOL-based predictive models of RSNs in NC and MCI, respectively; (c)-(d) show significantly decreased (blue) and increased (red) FC in MCI compared with NC (p=0.05).

respectively, showing that the predictive models of RSNs can reveal widespread FC alterations in MCI. For instance, the predicted DMN in MCI exhibits significantly decreased FC, as highlighted by the black boxes in Figs. 6a-6b. This is in agreement with previous study [7], but our studies revealed widespread FC alterations in MCI. In the future, we may use different levels of t thresholds to assess the connectivity difference between MCI and controls at the network-levels.

4 Conclusion

Due to the disruption of several RSNs in MCI, DICCCOLs that are structurally consistent in both NC and MCI were applied as predictive models of RSNs to assess FC alterations in MCI. Our results demonstrated that the predictive models of RSNs are effective and have revealed widespread FC alterations in MCI. In conclusion, we believe that the predictive models of RSNs offer a novel and effective solution to the challenging problem of accurately localizing corresponding network nodes ROIs in brain conditions for large-scale assessment of FC.

References

1. Stebbins, G.T., Murphy, C.M.: Diffusion tensor imaging in Alzheimer's disease and mild cognitive impairment. Behavioural Neurology 21(1), 39–49 (2009)
2. Dickerson, B.C., et al.: Large-scale functional brain network abnormalities in Alzheimer's disease: Insights from functional neuroimaging. Behav. Neurol. 21(1), 63–75 (2009)
3. Binnewijzend, M.A., et al.: Resting-state fMRI changes in Alzheimer's disease and mild cognitive impairment. Neurobiol. Aging 33(9), 2018–2028 (2012)
4. Beckmann, C.F., et al.: Investigations into resting-state connectivity using independent component analysis. Philos. Trans. R. Soc. Lond. B Biol. Sci. 360(1457), 1001–1013 (2005)
5. Zang, Y., et al.: Regional homogeneity approach to fMRI data analysis. NeuroImage 22(1), 394–400 (2004)
6. Zhang, T., et al.: Predicting functional cortical ROIs based on fiber shape models. Cerebral Cortex 22(4), 854–864 (2011)
7. Sorg, C., et al.: Selective changes of resting-state networks in individuals at risk for Alzheimer's disease. Proc. Natl. Acad. Sci. USA 104(47), 18760–18765 (2007)
8. `http://mialab.mrn.org/software/gift/index.html`
9. Zhu, D., et al.: DICCCOL: Dense Individualized and Common Connectivity-based Cortical Landmarks. Cerebral Cortex (2012), `http://dicccol.cs.uga.edu/`
10. Passingham, R.E., et al.: The anatomical basis of functional localization in the cortex. Nat. Rev. Neurosci. 3(8), 606–616 (2002)
11. Calhoun, V.D., et al.: A method for making group inferences from functional MRI data using independent component analysis. Hum. Brain Mapp. 14(3), 140–151 (2011)
12. Damoiseaux, J.S., et al.: Consistent resting-state networks across healthy subjects. Proc. Natl. Acad. Sci. USA 103(37), 13848–13853 (2006)
13. van den Heuvel, M., et al.: Normalized cut group clustering of resting-state FMRI data. PLoS One 3(4), e2001 (2008)
14. Li, K., et al.: Individual functional ROI optimization via maximization of group-wise consistency of structural and functional profiles. Neuroinformatics 10(3), 225–242 (2012)